

# Role of group velocity in tracking field energy in linear dielectrics

M. Ware, S. A. Glasgow, J. Peatross

*Dept. of Physics and Astronomy, Brigham Young University, Provo,  
UT 84602*

*mw22@email.byu.edu*

**Abstract:** A new context for the group delay function (valid for pulses of arbitrary bandwidth) is presented for electromagnetic pulses propagating in a uniform linear dielectric medium. The traditional formulation of group velocity is recovered by taking a narrowband limit of this generalized context. The arrival time of a light pulse at a point in space is defined using a time expectation integral over the Poynting vector. The delay between pulse arrival times at two distinct points consists of two parts: a spectral superposition of group delays and a delay due to spectral reshaping via absorption or amplification. The use of the new context is illustrated for pulses propagating both superluminally and subluminally. The inevitable transition to subluminal behavior for any initially superluminal pulse is also demonstrated.

© 2001 Optical Society of America

**OCIS codes:** (350.5500) Propagation; (260.2110) Electromagnetic Theory; (260.2030) Dispersion

---

## References and links

1. J. Peatross, S. A. Glasgow, and M. Ware, "Average Energy Flow of Optical Pulses in Dispersive Media," *Phys. Rev. Lett.* **84**, 2370-2373 (2000).
2. L. Brillouin, *Wave Propagation and Group Velocity* (Academic Press, New York, 1960).
3. M. Born and E. Wolf, *Principles of Optics*, 7th Ed. (Cambridge, 1999), pp. 19-24.
4. J. D. Jackson, *Classical Electrodynamics*, 3rd Ed. (Wiley, New York, 1998), pp. 323, 330-335.
5. R. Trebino, K. W. DeLong, D. N. Fittinghoff, J. N. Sweetser, M. A. Krumbugel, and B. A. Richman, "Measuring Ultrashort Laser Pulses in the Time-Frequency Domain Using Frequency-Resolved Optical Gating," *Rev. Sci. Instrum.* **68**, 3277-3295 (1997).
6. K. E. Oughstun and H. Xiao, "Failure of the Quasimonochromatic Approximation for Ultrashort Pulse Propagation in a Dispersive, Attenuative Medium," *Phys. Rev. Lett.* **78**, 642-645 (1997).
7. C. G. B. Garrett and D. E. McCumber, "Propagation of a Gaussian Light Pulse through an Anomalous Dispersion Medium," *Phys. Rev. A* **1**, 305-313 (1970).
8. R. Y. Chiao, "Superluminal (but Causal) Propagation of Wave Packets in Transparent Media with Inverted Atomic Populations," *Phys. Rev. A* **48**, R34-R37 (1993).
9. E. L. Bolda, J. C. Garrison, and R. Y. Chiao, "Optical Pulse Propagation at Negative Group Velocities due to a Nearby Gain Line," *Phys. Rev. A* **49**, 2938-2947 (1994).
10. R. Y. Chiao and A. M. Steinberg, "Tunneling Times and Superluminality," *Progress in Optics* **37**, pp. 347-406 (Emil Wolf ed., Elsevier, Amsterdam, 1997).
11. S. Chu and S. Wong, "Linear Pulse Propagation in an Absorbing Medium," *Phys. Rev. Lett.* **48**, 738-741 (1982).
12. L. J. Wang, A. Kuzmmich, and A. Dogariu, "Gain-Assisted Superluminal Light Propagation," *Nature* **406**, 277-279 (2000).
13. R. L. Smith, "The Velocities of Light," *Am. J. Phys.* **38**, 978-983 (1970).
14. M. Ware, W. E. Dibble, S. A. Glasgow, and J. Peatross, "Energy Flow in Angularly Dispersive Optical Systems," *J. Opt. Soc. Am. B* **18** 839-845 (2001) .
15. R. Loudon, "The Propagation of Electromagnetic Energy through an Absorbing Dielectric," *J. Phys. A* **3**, 233-245 (1970).
16. Md. Aminul Islam Talukder, Yoshimitsu Amagishi, and Makoto Tomita, "Superluminal to Subluminal Transition in the Pulse Propagation in a Resonantly Absorbing Medium," *Phys. Rev. Lett.* **86**, 3546-3549 (2001).

## 1 Introduction

We recently introduced [1] a context wherein the group delay function always retains meaning for electromagnetic pulses propagating in linear homogeneous media. This includes broadband pulses with arbitrarily complicated temporal structure and with spectra in regions of anomalous dispersion. The context we provide differs from traditional pedagogy [2, 3, 4] wherein group velocity has been understood within a strict narrowband limit. (The new context has increasing experimental relevance since ultrashort laser pulses are routinely generated and characterized in the laboratory [5].) In this article, we provide further details regarding this context, including a full derivation.

Before proceeding, we briefly review the solutions of Maxwell’s equation and how they relate to the traditional understanding of group delay [4]. In a linear, non-magnetic, non-conducting medium Maxwell’s equations can be written as

$$\nabla \times \mathbf{E}(\mathbf{r}, t) + \frac{\partial \mathbf{B}(\mathbf{r}, t)}{\partial t} = 0, \quad (1)$$

$$\nabla \times \frac{\mathbf{B}(\mathbf{r}, t)}{\mu_0} - \epsilon_0 \frac{\partial \mathbf{E}(\mathbf{r}, t)}{\partial t} = \frac{\partial \mathbf{P}(\mathbf{r}, t)}{\partial t}. \quad (2)$$

The usual method of obtaining solutions to these equations in a homogeneous medium is to select points in space and consider the time behavior of the pulse at each point. The frequency domain and time domain representation of the electric field  $\mathbf{E}$  at a point  $\mathbf{r}$  are related by

$$\mathbf{E}(\mathbf{r}, \omega) = \frac{1}{\sqrt{2\pi}} \int_{-\infty}^{\infty} e^{i\omega t} \mathbf{E}(\mathbf{r}, t) dt, \quad (3)$$

$$\mathbf{E}(\mathbf{r}, t) = \frac{1}{\sqrt{2\pi}} \int_{-\infty}^{\infty} e^{-i\omega t} \mathbf{E}(\mathbf{r}, \omega) d\omega. \quad (4)$$

Analogous expressions for  $\mathbf{P}$  and  $\mathbf{B}$  give the time/frequency connection for the polarization and magnetic field. In our convention, we take all fields to be real in the time domain, so the following symmetry holds in the frequency domain:

$$\mathbf{E}(\mathbf{r}, -\omega) = \mathbf{E}^*(\mathbf{r}, \omega) \quad (5)$$

(with analogous expressions for  $\mathbf{B}$  and  $\mathbf{P}$ ).

In the frequency domain, Maxwell’s equations have as a solution

$$\mathbf{E}(\mathbf{r}_0 + \Delta\mathbf{r}, \omega) = \mathbf{E}(\mathbf{r}_0, \omega) e^{i\mathbf{k} \cdot \Delta\mathbf{r}}, \quad (6)$$

where the initial pulse form  $\mathbf{E}(\mathbf{r}_0, \omega)$  is chosen at a point  $\mathbf{r}_0$ . The solution renders the pulse form  $\mathbf{E}(\mathbf{r}_0 + \Delta\mathbf{r}, \omega)$  (in terms of the initial pulse form) at any other point shifted by the displacement  $\Delta\mathbf{r}$ . (Implicit in (6) is the restricting assumption that each frequency is associated with a single wave vector  $\mathbf{k}(\omega)$ , although the wave vectors need not be all in the same direction.) The magnetic field is obtained in terms of the electric field through

$$\mathbf{B}(\mathbf{r}, \omega) = \mathbf{k}(\omega) \times \mathbf{E}(\mathbf{r}, \omega) / \omega. \quad (7)$$

In accordance with the linear, isotropic, and homogeneous assumptions, the susceptibility  $\chi(\omega)$  defines the (temporally non-local, but frequency local) constitutive relation between the electric field and the polarization:

$$\mathbf{P}(\mathbf{r}, \omega) = \epsilon_0 \chi(\omega) \mathbf{E}(\mathbf{r}, \omega). \quad (8)$$

Maxwell's equations together with (8) also impose the constraint

$$k^2(\omega) = \frac{\omega^2}{c^2} [1 + \chi(\omega)]. \quad (9)$$

Here we take the traditional vantage point of considering the frequency  $\omega$  to be real, whereas the wave vector  $\mathbf{k}(\omega)$  can be complex when the susceptibility  $\chi(\omega)$  is complex.

In order to obtain the temporal profile of the pulse, the solution (6) must be transformed to the time domain via (4). The traditional concept of group velocity is obtained by expanding the frequency-dependent phase delay as

$$\mathbf{k}(\omega) \cdot \Delta \mathbf{r} \approx [\mathbf{k}|_{\bar{\omega}} \cdot \Delta \mathbf{r}] + \left[ \frac{\partial \mathbf{k}}{\partial \omega} \Big|_{\bar{\omega}} \cdot \Delta \mathbf{r} \right] (\omega - \bar{\omega}) + \dots \quad (10)$$

before carrying out the inverse transform. After performing the inverse transform with this approximate phase delay, the real part of the coefficient of the linear frequency term is seen to give (to first order) the time required for the pulse to traverse the displacement  $\Delta \mathbf{r}$ . The function  $\partial \text{Re } \mathbf{k} / \partial \omega \cdot \Delta \mathbf{r}$  is known as the *group delay function*, and in the traditional context is evaluated at a single ‘carrier’ frequency  $\bar{\omega}$ . Group velocity is obtained by dividing the displacement  $\Delta \mathbf{r}$  by the group delay function evaluated at  $\bar{\omega}$ .

The failings of (10) are well documented [6]. In particular, if the bandwidth of an electromagnetic pulse encompasses a substantial portion of a resonance structure, it becomes necessary to retain a large number of terms in the expansion (10) to accurately describe the phase delay. Moreover, as was pointed out by Garret and McCumber [7], if the bandwidth exceeds the modulus of the difference between the carrier frequency and the nearest pole in the refractive index, the series fails to converge altogether. Because of these difficulties, textbooks on the subject state that the traditional concept of group velocity “has no longer any appreciable physical significance” [3] or “may even lack precise meaning” [4] in these situations. In this article (see also [1]), we endeavor to supply this “precise meaning” that has been absent in the broadband context. In particular, we demonstrate that the time required for a pulse to traverse a displacement  $\Delta \mathbf{r}$  is described by a *linear superposition of group delays, weighted by the surviving spectral content of the pulse*. Mathematically, this delay is given by

$$\Delta t_G(\mathbf{r}) = \int_{-\infty}^{\infty} \rho(\mathbf{r}, \omega) \left( \frac{\partial \text{Re } \mathbf{k}}{\partial \omega} \cdot \Delta \mathbf{r} \right) d\omega, \quad (11)$$

where  $\rho(\mathbf{r}, \omega)$  is a normalized spectral distribution of Poynting flux (at the final point) defined by

$$\rho(\mathbf{r}, \omega) \equiv \hat{\eta} \cdot \mathbf{S}(\mathbf{r}, \omega) \Big/ \hat{\eta} \cdot \int_{-\infty}^{\infty} \mathbf{S}(\mathbf{r}, \omega) d\omega. \quad (12)$$

( $\hat{\eta}$  is a unit vector normal to the detector surface.) Another delay term due to spectral reshaping also plays a role in determining the total delay time. This additional delay term, which is evaluated without propagation, becomes important when an initially chirped pulse undergoes an alteration in its spectral profile. For an unchirped pulse, the reshaping effect is generally negligible. No approximations or expansions of the type (10) are used in the new formulation, making the results general.

We note that the fact that group velocity can become superluminal and/or negative in the vicinity of a resonance structure does not indicate a failure of the expansion (10) [7, 8, 9, 10]. This type of exotic behavior (well verified experimentally [11, 12]) occurs in a narrowband limit. The context we present describes the gradual (and inevitable)

transition from superluminal to subluminal behavior as the initial temporal profile of a pulse becomes more sharply defined, and the expansion (10) cannot be used. Since the new formalism is exact, the extreme broadband limit can also be taken which leads to the well-known Sommerfeld-Brillouin [2] result that a sharply defined signal travels at exactly  $c$ , the speed of light in vacuum.

## 2 Average arrival time of poynting flux to a point

In order to concretely discuss the time required for a pulse to traverse a given displacement, we first define the arrival time of a pulse to a point (say where a detector is located). This definition need only involve the Poynting vector, since it alone transports energy. To deal with arbitrary broadband pulses, the arrival time should avoid presupposing a specific pulse shape, since the pulse may evolve in complicated ways during propagation. For example, the peak or the midpoint on the rising edge of a pulse is a poor indicator of arrival time if the pulse contains multiple peaks or a long and non-uniform rise time.

For the reasons given, we use a time expectation integral (proposed by Smith in 1970 [13]) to specify the arrival of the pulse:

$$\langle t \rangle_{\mathbf{r}} \equiv \int_{-\infty}^{\infty} t \rho(\mathbf{r}, t) dt, \quad (13)$$

where  $\rho(\mathbf{r}, t)$  is a normalized temporal distribution of the Poynting flux at  $\mathbf{r}$ :

$$\rho(\mathbf{r}, t) \equiv \hat{\eta} \cdot \mathbf{S}(\mathbf{r}, t) / \hat{\eta} \cdot \int_{-\infty}^{\infty} \mathbf{S}(\mathbf{r}, t) dt. \quad (14)$$

The Poynting vector is defined as usual:

$$\mathbf{S}(\mathbf{r}, t) \equiv \mathbf{E}(\mathbf{r}, t) \times \frac{\mathbf{B}(\mathbf{r}, t)}{\mu_0}. \quad (15)$$

As Smith explained, this definition “is not restricted to a quasi monochromatic pulse or to a situation which one has always only a single pulse. ... It yields a unique value regardless of the dispersion present.” The unit vector  $\hat{\eta}$  refers to the direction in which the energy flow is detected (normal to a detector surface). It has importance for angularly dispersive systems such as grating pairs used for pulse compression where the result of the integral in the numerator is not necessarily parallel to that in the denominator. We have addressed the angularly dispersive case elsewhere [14].

Motivated by a desire to make connection with the traditional group velocity, we rewrite the arrival time (13) of the pulse in terms of the frequency representations of the fields involved. The denominator of (14) may be transformed immediately via Parseval’s theorem:

$$\int_{-\infty}^{\infty} \mathbf{S}(\mathbf{r}, t) dt = \int_{-\infty}^{\infty} \mathbf{S}(\mathbf{r}, \omega) d\omega, \quad (16)$$

where the frequency representation of the Poynting vector is given by:

$$\mathbf{S}(\mathbf{r}, \omega) \equiv \mathbf{E}(\mathbf{r}, \omega) \times \frac{\mathbf{B}^*(\mathbf{r}, \omega)}{\mu_0}. \quad (17)$$

Employing the Fourier relations (3) and (4) in the numerator of (13) (with (14) inserted), we find

$$\begin{aligned} \int_{-\infty}^{\infty} t \mathbf{S}(\mathbf{r}, t) dt &= \int_{-\infty}^{\infty} t \left[ \frac{1}{\sqrt{2\pi}} \int_{-\infty}^{\infty} \mathbf{E}(\mathbf{r}, \omega) e^{-i\omega t} d\omega \right] \\ &\quad \times \left[ \frac{1}{\sqrt{2\pi}} \int_{-\infty}^{\infty} \mathbf{B}(\mathbf{r}, \omega') e^{-i\omega' t} d\omega' \right] dt. \end{aligned} \quad (18)$$

By introducing a frequency derivative to account for the factor  $t$ , the expression (18) can be recast as

$$\int_{-\infty}^{\infty} t \mathbf{S}(\mathbf{r}, t) dt = i \int_{-\infty}^{\infty} d\omega \mathbf{E}(\mathbf{r}, \omega) \times \frac{\partial}{\partial \omega} \left[ \int_{-\infty}^{\infty} d\omega' \frac{\mathbf{B}(\mathbf{r}, \omega')}{\mu_0} \frac{1}{2\pi} \int_{-\infty}^{\infty} e^{-i(\omega+\omega')t} dt \right]. \quad (19)$$

The final integral is recognized as a delta function, which permits the integration over  $\omega'$  to be performed:

$$\begin{aligned} \int_{-\infty}^{\infty} t \mathbf{S}(\mathbf{r}, t) dt &= i \int_{-\infty}^{\infty} \mathbf{E}(\mathbf{r}, \omega) \times \frac{\partial}{\partial \omega} \frac{\mathbf{B}(\mathbf{r}, -\omega)}{\mu_0} d\omega \\ &= -i \int_{-\infty}^{\infty} \frac{\partial \mathbf{E}(\mathbf{r}, \omega)}{\partial \omega} \times \frac{\mathbf{B}^*(\mathbf{r}, \omega)}{\mu_0} d\omega. \end{aligned} \quad (20)$$

Here we have invoked the symmetry relation (5). We have also integrated by parts in order to place (by preference) the derivative on the electric field rather than on the magnetic field. In doing this, we have assumed a pulse of a finite duration. Equations (16) and (20) lead to the frequency domain representation of the arrival time:

$$\langle t \rangle_{\mathbf{r}} = T[\mathbf{E}(\mathbf{r}, \omega)], \quad (21)$$

where

$$T[\mathbf{E}(\mathbf{r}, \omega)] \equiv -i \hat{\eta} \cdot \int_{-\infty}^{\infty} \frac{\partial \mathbf{E}(\mathbf{r}, \omega)}{\partial \omega} \times \frac{\mathbf{B}^*(\mathbf{r}, \omega)}{\mu_0} d\omega \Big/ \hat{\eta} \cdot \int_{-\infty}^{\infty} \mathbf{S}(\mathbf{r}, \omega) d\omega. \quad (22)$$

In (22) we have indicated that the function  $T$  depends only on the electric field since the magnetic field can be written in terms of the electric field through (7).

### 3 Delay time between two points

The arrival time of the pulse as expressed in (22) is not very useful in itself. Its usefulness is revealed when applied to the difference in arrival times of a pulse to two different locations, say  $\mathbf{r}_0$  and  $\mathbf{r} = \mathbf{r}_0 + \Delta\mathbf{r}$ . The difference in the arrival times of the two points is defined as

$$\Delta t \equiv \langle t \rangle_{\mathbf{r}} - \langle t \rangle_{\mathbf{r}_0} = T[\mathbf{E}(\mathbf{r}_0 + \Delta\mathbf{r}, \omega)] - T[\mathbf{E}(\mathbf{r}_0, \omega)]. \quad (23)$$

Our goal in this section is to recast (23) into a form that makes clear the connection between  $\Delta t$  and the group delay function  $\partial \text{Re } \mathbf{k} / \partial \omega \cdot \Delta\mathbf{r}$ .

In order to arrive at the desired result, we first obtain an explicit form for  $T[\mathbf{E}(\mathbf{r}_0 + \Delta\mathbf{r}, \omega)]$ . With the solution (6) we can evaluate the integrand of the numerator of (22) at  $\mathbf{r}_0 + \Delta\mathbf{r}$  as follows:

$$\begin{aligned} \frac{\partial \mathbf{E}(\mathbf{r}_0, \omega) e^{i\mathbf{k} \cdot \Delta\mathbf{r}}}{\partial \omega} \times \frac{\mathbf{B}^*(\mathbf{r}_0, \omega) e^{-i\mathbf{k}^* \cdot \Delta\mathbf{r}}}{\mu_0} &= i \frac{\partial \text{Re } \mathbf{k} \cdot \Delta\mathbf{r}}{\partial \omega} \mathbf{E}(\mathbf{r}_0, \omega) \times \mathbf{B}^*(\mathbf{r}_0, \omega) e^{-2 \text{Im } \mathbf{k} \cdot \Delta\mathbf{r}} \\ &\quad + \frac{\partial \mathbf{E}(\mathbf{r}_0, \omega) e^{-\text{Im } \mathbf{k} \cdot \Delta\mathbf{r}}}{\partial \omega} \times \frac{\mathbf{B}^*(\mathbf{r}_0, \omega) e^{-\text{Im } \mathbf{k} \cdot \Delta\mathbf{r}}}{\mu_0}. \end{aligned} \quad (24)$$

The integrand of the denominator in (22) is also evaluated at  $\mathbf{r}_0 + \Delta\mathbf{r}$ , giving

$$\begin{aligned} \mathbf{S}(\mathbf{r}_0 + \Delta\mathbf{r}, \omega) &= \mathbf{E}(\mathbf{r}_0, \omega) e^{i\mathbf{k} \cdot \Delta\mathbf{r}} \times \frac{\mathbf{B}^*(\mathbf{r}_0, \omega) e^{-i\mathbf{k}^* \cdot \Delta\mathbf{r}}}{\mu_0} \\ &= \mathbf{E}(\mathbf{r}_0, \omega) e^{-\text{Im } \mathbf{k} \cdot \Delta\mathbf{r}} \times \frac{\mathbf{B}^*(\mathbf{r}_0, \omega) e^{-\text{Im } \mathbf{k}^* \cdot \Delta\mathbf{r}}}{\mu_0}. \end{aligned} \quad (25)$$

Upon using (24) and (25) with the arrival time (22) we obtain

$$T[\mathbf{E}(\mathbf{r}_0 + \Delta\mathbf{r}, \omega)] = \frac{\hat{\eta} \cdot \int_{-\infty}^{\infty} \mathbf{S}(\mathbf{r}, \omega) \left( \frac{\partial \text{Re} \mathbf{k}}{\partial \omega} \cdot \Delta\mathbf{r} \right) d\omega}{\hat{\eta} \cdot \int_{-\infty}^{\infty} \mathbf{S}(\mathbf{r}, \omega) d\omega} - i \frac{\hat{\eta} \cdot \int_{-\infty}^{\infty} \frac{\partial \mathbf{E}(\mathbf{r}_0, \omega) e^{-\text{Im} \mathbf{k} \cdot \Delta\mathbf{r}}}{\partial \omega} \times \frac{\mathbf{B}^*(\mathbf{r}_0, \omega) e^{-\text{Im} \mathbf{k}^* \cdot \Delta\mathbf{r}}}{\mu_0} d\omega}{\hat{\eta} \cdot \int_{-\infty}^{\infty} e^{-2\text{Im} \mathbf{k} \cdot \Delta\mathbf{r}} \mathbf{S}(\mathbf{r}_0, \omega) d\omega}. \quad (26)$$

Using the expressions (22) and (26), we can now write the delay time (23) as the sum of two intuitive terms:

$$\Delta t = \Delta t_G(\mathbf{r}) + \Delta t_R(\mathbf{r}_0). \quad (27)$$

The first term in (27), the *net group delay*, is a spectral average of the group delay function over the spectral intensity that is experienced at the final point  $\mathbf{r}$  (as already mentioned in connection with ):

$$\Delta t_G(\mathbf{r}) = \int_{-\infty}^{\infty} \rho(\mathbf{r}, \omega) \left( \frac{\partial \text{Re} \mathbf{k}}{\partial \omega} \cdot \Delta\mathbf{r} \right) d\omega, \quad (28)$$

where we have defined a normalized spectral distribution of field energy:

$$\rho(\mathbf{r}, \omega) \equiv \hat{\eta} \cdot \mathbf{S}(\mathbf{r}, \omega) \Big/ \hat{\eta} \cdot \int_{-\infty}^{\infty} \mathbf{S}(\mathbf{r}, \omega) d\omega. \quad (29)$$

Note the close resemblance between (13) and (28). Both are expectation integrals, the former being executed as a ‘center of mass’ integral in time, the later being executed in the frequency domain on  $\partial \text{Re} \mathbf{k} / \partial \omega \cdot \Delta\mathbf{r}$ . Clearly, the group delay function evaluated at every frequency present in the pulse influences the result. The net group delay depends only on the spectral content of the pulse, independent of its temporal organization (i.e. the phases of  $\mathbf{E}(\mathbf{r}, \omega)$  and  $\mathbf{B}(\mathbf{r}, \omega)$  do not contribute). Only the real part of  $\mathbf{k}$  plays a direct role in (28).

The second term in (27) represents a delay which arises solely from a reshaping of the spectrum through absorption (or amplification) and is given by

$$\Delta t_R(\mathbf{r}_0) \equiv T[e^{-\text{Im} \mathbf{k} \cdot \Delta\mathbf{r}} \mathbf{E}(\mathbf{r}_0, \omega)] - T[\mathbf{E}(\mathbf{r}_0, \omega)]. \quad (30)$$

This reshaping delay is evaluated at  $\mathbf{r}_0$ , *before* propagation takes place. The reshaping delay is the difference between the pulse arrival time at the initial point  $\mathbf{r}_0$  evaluated *without* and *with* the spectral amplitude that will be lost (or gained) during propagation. Both terms in (30) utilize the phase of the fields at  $\mathbf{r}_0$ . Thus, in contrast to the net group delay, the reshaping delay is sensitive to how the pulse is organized. The reshaping delay is zero if the spectral amplitude of the pulse is unaltered during propagation (i.e. if the imaginary part of  $\mathbf{k}$  can be neglected). The reshaping delay is also relatively unimportant if the pulse is unchirped before propagation and in the narrowband limit even if pulses experience strong absorption (or amplification).

Before proceeding, it is interesting to note that in (27) the ordering for the evaluation of the net group delay and reshaping delay can be reversed. In other words, the arguments  $\mathbf{r}$  and  $\mathbf{r}_0$  in (27) can be interchanged which gives

$$\Delta t_G(\mathbf{r}) + \Delta t_R(\mathbf{r}_0) = \Delta t_G(\mathbf{r}_0) + \Delta t_R(\mathbf{r}). \quad (31)$$

This commutative property can dramatically alter the group and reshaping delays taken individually. Nevertheless, their sum  $\Delta t$  is unaffected by the ordering. The group delay

computed over the initial spectrum is

$$\Delta t_G(\mathbf{r}_0) = \int_{-\infty}^{\infty} \rho(\mathbf{r}_0, \omega) \left( \frac{\partial \text{Re } \mathbf{k}}{\partial \omega} \cdot \Delta \mathbf{r} \right) d\omega. \quad (32)$$

When the group delay is computed using the initial spectrum before the propagation, the reshaping delay is evaluated at the end of propagation without and with the lost spectral amplitude:

$$\Delta t_R(\mathbf{r}) = T[\mathbf{E}(\mathbf{r}_0 + \Delta \mathbf{r}, \omega)] - T[e^{\text{Im } \mathbf{k} \cdot \Delta \mathbf{r}} \mathbf{E}(\mathbf{r}_0 + \Delta \mathbf{r}, \omega)]. \quad (33)$$

In this expression, the initial spectral amplitude is restored to the second term. The proof of (31) is straightforward. Directly by substitution into (26) we have

$$\begin{aligned} T[e^{\text{Im } \mathbf{k} \cdot \mathbf{r}} \mathbf{E}(\mathbf{r}_0 + \Delta \mathbf{r}, \omega)] &= \frac{\hat{\eta} \cdot \int_{-\infty}^{\infty} \mathbf{S}(\mathbf{r}_0, \omega) \left( \frac{\partial \text{Re } \mathbf{k}}{\partial \omega} \cdot \Delta \mathbf{r} \right) d\omega}{\hat{\eta} \cdot \int_{-\infty}^{\infty} \mathbf{S}(\mathbf{r}_0, \omega) d\omega} \\ &\quad - i \frac{\hat{\eta} \cdot \int_{-\infty}^{\infty} \frac{\partial \mathbf{E}(\mathbf{r}_0, \omega)}{\partial \omega} \times \frac{\mathbf{B}^*(\mathbf{r}_0, \omega)}{\mu_0} d\omega}{\hat{\eta} \cdot \int_{-\infty}^{\infty} \mathbf{S}(\mathbf{r}_0, \omega) d\omega} \end{aligned} \quad (34)$$

When this and (26) are used in (33), the commutative relationship (31) is immediately verified.

The expression (27) gives the delay between the ‘center of mass’ arrival times for any two points in a medium regardless of how the pulse evolves during transit. Since the form is obtained without approximation, it is valid for arbitrary bandwidths. This formalism does not attempt to define a specific “group velocity” as being representative of the overall pulse propagation, since in general propagation velocity need not be constant. Rather we have demonstrated that the delay between arrival times at two points is related to a linear superposition of group delays weighted by the pulse’s spectral content (i.e. equation (28)). By taking the limit of small separation a local velocity can be defined at each point along the propagation [13]. However, we prefer to consider the difference in arrival times at two discretely separated points since this is more directly applicable to experiment.

Of course in the narrowband limit we expect the delay time to give the traditional result presented in section 1. In this limit the reshaping delay tends to zero so that the total delay is dominated by the net group delay. The normalized spectral distribution approaches a delta function ( $\rho(\omega) \rightarrow \delta(\omega - \bar{\omega})$ ) so that the total delay reduces to  $\Delta t \rightarrow \Delta t_G = \partial \text{Re } \mathbf{k} / \partial \omega|_{\bar{\omega}} \cdot \Delta \mathbf{r}$ . This is in agreement with the well verified observation [7, 8, 9, 10, 11] that a pulse travels at the group velocity evaluated at  $\bar{\omega}$  in the narrowband limit.

#### 4 The effect of pulse bandwidth on delay time

The use of (27) has been illustrated elsewhere [1] for both narrowband and broadband pulses in an absorptive medium. Here, we illustrate the use of the theorem in an amplifying medium. We employ the Lorentz model with a single resonance at  $\omega_0$  and a damping frequency  $\gamma$ . (Note that the previous results are independent of any specific model.) In accordance with the model, the linear susceptibility is  $\chi(\omega) = f\omega_p^2 / (\omega_0^2 - \omega^2 - i\gamma\omega)$ , where  $\omega_p$  is the plasma frequency and  $f$  is the oscillator strength, which is negative for an inverted medium [9]. Figure 1(a) depicts the real and imaginary parts of the index where we have chosen the model parameters to be  $\omega_0 = 100\gamma$  and  $f\omega_p^2 = -100\gamma^2$ . The real and imaginary parts of the index are related to the susceptibility through

$$[\text{Re } n(\omega) + i \text{Im } n(\omega)]^2 = 1 + \chi(\omega) \quad (35)$$

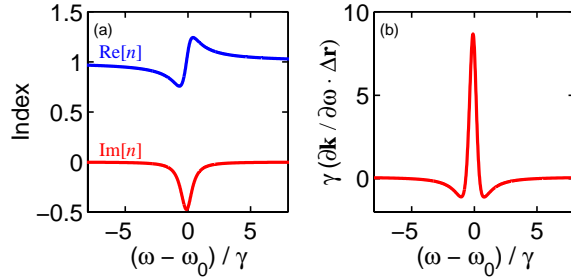


Fig. 1. (a) Real and imaginary parts of the refractive index. (b) Group delay function for the given index

For simplicity, we consider propagation in only one dimension, so that  $\mathbf{k} = k\hat{z}$ . We will consider the delay time of a pulse as it propagates through a displacement  $\Delta\mathbf{r} = 0.1(c/\gamma)\hat{z}$ . Figure 1(b) depicts the group delay function  $\partial\mathbf{k}/\partial\omega \cdot \Delta\mathbf{r}$  for these parameters.

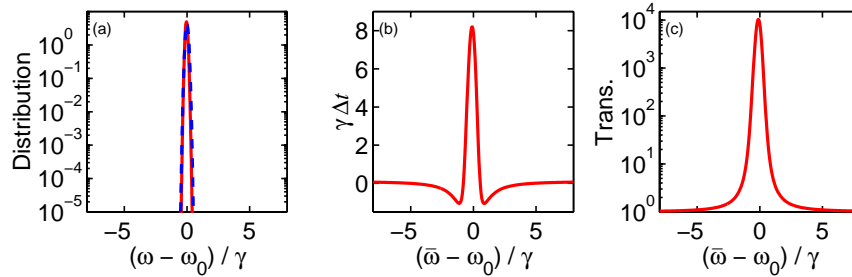


Fig. 2. (a) Normalized spectral distribution  $\rho$  for the narrowband pulse centered on resonance before (dotted) and after (solid) propagation. (b) Total delay as a function of  $\bar{\omega}$  for the narrowband pulse. (c) Overall pulse transmission as a function of  $\bar{\omega}$

The electric field at  $\mathbf{r}_0$  is chosen to be Gaussian,  $\mathbf{E}(\mathbf{r}_0, t) = \hat{x}\mathbf{E}_0\exp(-t^2/\tau^2)\cos(\bar{\omega}t)$ , with initial duration  $\tau = 10/\gamma$ . In all of the following examples the pulses are initially unchirped, so that the reshaping delay  $\Delta t_R$  is negligible. Figure 2(a) depicts the normalized spectral distribution function (Eq. (29)) of the narrowband pulse before (dotted line) and after (solid line) propagation in the medium, with the initial spectrum centered on resonance (i.e.  $\bar{\omega} = \omega_0$ ). Because the initial pulse spectrum is narrow compared to the resonance,  $\rho$  changes little during propagation. Since the reshaping delay is negligible, the total delay time is given by the expectation of the group delay function (shown in Fig. 1(b)) weighted by the spectral distribution (shown in Fig. 2(a)) as in Eq. (28). Figure 2(b) plots the delay time as the pulse's central frequency  $\bar{\omega}$  is varied relative to the resonance frequency  $\omega_0$ . Since  $\rho(\mathbf{r}, \omega)$  is narrow compared to the width of the resonance, the total delay closely resembles the group delay function in Fig. 2(b). Figure 2(c) plots the ratio of the pulse energy after propagation to that before propagation as the pulse's central frequency is varied.

Fig. 3 repeats Fig. 2 for the case of the broadband pulse. Note that in the broadband case, the negative delay times seen in Fig. 2(b) disappear. This illustrates the general principle that superluminal effects are a narrowband phenomenon which disappears as bandwidth is increased.

The difference between the narrowband and broadband examples just discussed can be clearly seen when one constructs the spatial profile of the pulses' field energy using the methods summarized in the introduction. Figure 4 is an animation of the narrowband



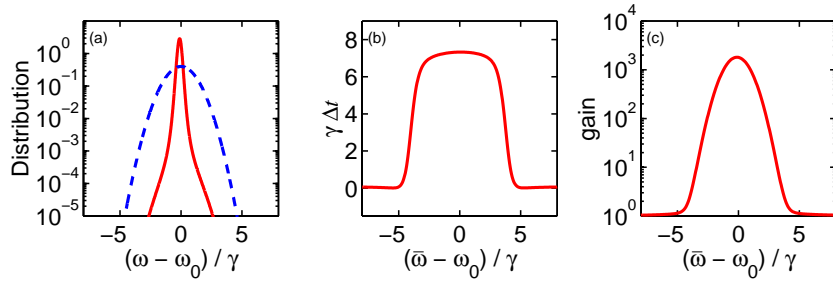


Fig. 3. (a) Normalized spectral distribution  $\rho$  for the broadband pulse centered on resonance before (dotted) and after (solid) propagation. (b) Total delay as a function of  $\bar{\omega}$  for the broadband pulse. (c) Overall pulse transmission as a function of  $\bar{\omega}$

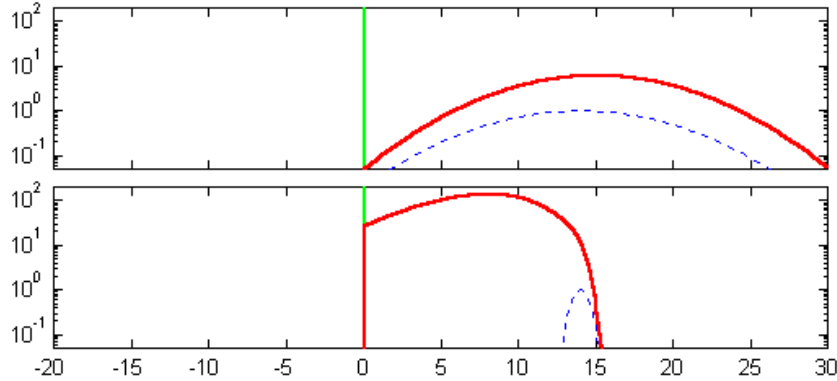


Fig. 4. Animation of narrowband (top) and broadband (bottom) gaussian pulses traversing an amplifying medium (1.4 MB)

(top) and broadband (bottom) pulses from Figs. 2 and 3 as they traverse the amplifying medium (represented by the vertical bar). For this illustration we have centered the bandwidth of the pulses at  $\bar{\omega} - \omega_0 = \gamma$  where the pulse in Fig. 2 exhibits the most dramatic superluminal behavior. The dotted line represents the pulse as it would have travelled in vacuum and the solid line indicates the actual pulse profile. In the animation it is clear that the centroid of the narrowband pulse is shifted forward relative to the vacuum pulse upon traversing the medium. In contrast, the broadband pulse is delayed relative to the vacuum pulse.

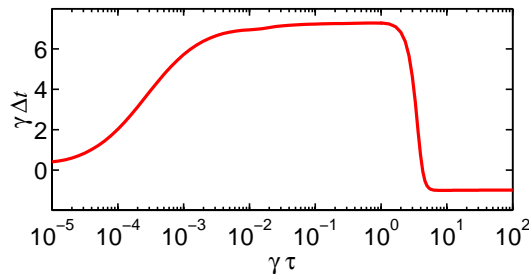


Fig. 5. Total delay as the width of the pulse is changed from broadband to narrowband.

We now illustrate the transition from superluminal to subluminal delay times as the pulse bandwidth increases. For this example we use the medium described in relation to Fig. 1 and center the bandwidth of the pulse at  $\bar{\omega} - \omega_0 = \gamma$ . Figure 5 plots the

delay time as the pulse duration  $\tau$  (and hence the bandwidth) is varied. As expected, the pulses with narrow bandwidths (large  $\tau$ ) exhibit superluminal effects. The behavior becomes subluminal as the bandwidth increases ( $\tau$  decreases). This is easily understood in terms of (28). As the bandwidth increases,  $\rho(\mathbf{r}, \omega)$  includes more and more of the ‘slow’ spectral components near  $\omega_0$ . When the expectation (28) is taken, these ‘slow’ spectral components outweigh the effect of the frequencies with a negative group delay function resulting in a subluminal delay time.

As the pulse duration goes to zero in Fig. 5, the total delay time decreases and approaches an exactly luminal delay time. This behavior can be clearly explained using the context developed in sections 2–3. When the duration of the pulse goes to zero, becoming a delta function in time, the spectral content of the pulse extends uniformly over all frequencies ( $\rho(\omega) \rightarrow \text{constant}$ ). By comparison, any resonance structure encompasses a finite bandwidth, and the reshaping delay tends to zero. If, for simplicity, we consider all wave vectors to be parallel (i.e.  $\mathbf{k}(\omega) = k(\omega) \hat{k}$ ) we have from (28) or (32) that  $\Delta t \rightarrow \Delta t_G \approx \text{Re} \mathbf{k}/\omega|_{\infty} \cdot \Delta \mathbf{r} = \hat{k} \cdot \Delta \mathbf{r}/c$ , assuming a refractive index which approaches unity at high frequency. This demonstrates (without lengthy analyses or numerical simulations) the well-known fact that the velocity for a sharply defined signal is exactly  $c$ . Thus, the Sommerfeld-Brillouin result [2] of luminality for pulses of definite support is consistent with and even implied by the present context.

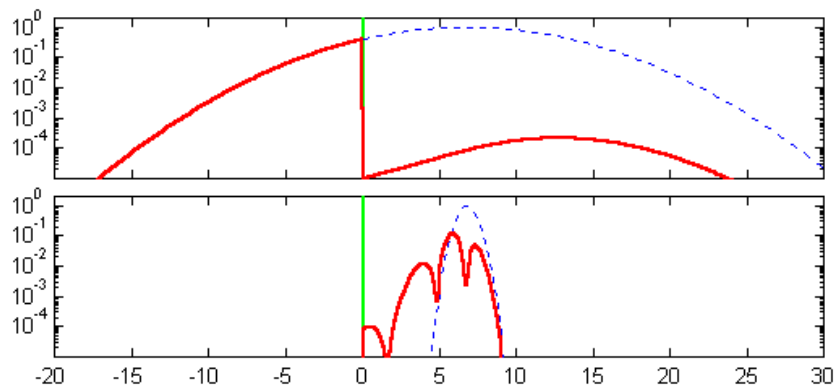


Fig. 6. Animation of narrowband (top) and broadband (bottom) gaussian pulses traversing an absorbing medium (1.7 MB)

As has been known for several decades [7, 11, 4], superluminal effects are also observed in absorbing dielectric media. In an absorbing medium, the group delay function is similar to that plotted in Fig. 2(b), except it is inverted (i.e. the group delay function is negative near resonance and becomes positive away from resonance). Thus, in an absorbing medium pulses whose spectra are centered on resonance exhibit the most dramatic superluminal delay times. Here again, if the pulse’s spectrum is too broad, the effects of the slow off-resonance spectral components in  $\rho(\mathbf{r}, \omega)$  will outweigh the on resonance components resulting in luminal delay times. Figure 6 is an animation illustrating the difference between narrowband and broadband pulses in an absorbing medium. The pulse parameters are the same as in fig. 4, and the medium parameters are the same except  $f = +1$  in order to make an absorbing medium. (These parameters are identical to those used in [1].) Again it is the narrowband pulse that is seen to be advanced relative to the vacuum pulse.

## 5 Propagation distance and delay time

Although we have demonstrated that superluminal behavior is most pronounced for narrowband pulses, when  $\Delta \mathbf{r}$  is small enough it is possible to observe superluminal effects for broadband pulses. This was demonstrated recently by Talukder and coworkers [16] when they performed a superluminal propagation experiment in an absorbing medium under relatively broadband conditions (where the traditional narrowband expansion of group velocity fails). Although their femtosecond laser pulses initially propagated superluminally through a dye cell, as the effective length of the propagation medium was increased, they observed a transition to subluminal behavior. The formalism developed in the present paper may be used to explain why this transition inevitably occurs as an initially superluminal pulse is allowed to propagate longer distances in an absorbing medium.

If the pulse is initially unchirped, the reshaping delay  $\Delta t_R(\mathbf{r}_0)$  is negligible, so that the total delay is given by  $\Delta t_G(\mathbf{r})$ . When the pulse spectrum is centered on-resonance,  $\rho(\mathbf{r}, \omega)$  will primarily include the ‘fast’ spectral components near  $\omega_0$  (remember that in an absorbing medium, frequencies near  $\omega_0$  have the shortest group delay function). However, as it travels, the fast spectral components near  $\omega_0$  are absorbed from the pulse spectrum. Eventually only spectral components away from the resonance (i.e. frequencies where the group delay function gives a luminal delay) are left in the spectrum. The delay time, given by the net group delay (28), then becomes subluminal.

The situation in an amplifying medium is similar. In this case, it is the off resonance frequency components that have the superluminal group delay. As the pulse propagates, the amplifying medium adds the slow near-resonance frequencies to the pulse spectrum. Thus, an initially superluminal pulse whose spectrum is centered off-resonance will eventually have a luminal delay time as  $\rho(\mathbf{r}, \omega)$  changes to include more near-resonance frequencies.

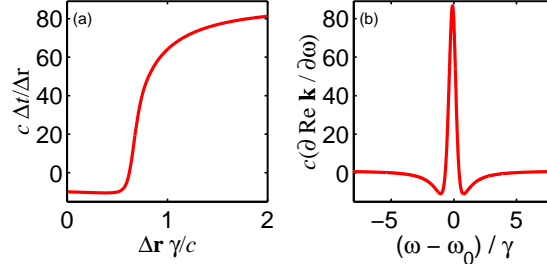


Fig. 7. (a) Total delay, scaled by  $c/\Delta r$ , as a function of displacement. (b) The group delay function divided by displacement.

To illustrate this transition to luminal delay times as propagation distance is increased, Figure 7(a) plots delay time as a function of displacement in an amplifying medium (medium parameters are the same as in Fig. 1 except for the variable displacement). The initial pulse is chosen to be a narrowband gaussian as in fig. 2, with  $\tau = 10/\gamma$  and  $\bar{\omega} - \omega_0 = 1\gamma$ . For ease of comparison, the delay time is scaled by  $c/\Delta \mathbf{r}$  so that propagation at the speed of light has a scaled delay time of 1. Figure 7 (b) shows the group delay function (also scaled by  $c/\Delta \mathbf{r}$ ). For small displacements, the delay time matches the group delay function evaluated at  $\bar{\omega}$ . As the pulse propagates and acquires more on-resonance spectral intensity, the delay time shifts to the on-resonance value of the group delay function.

The preceding example illustrates the principle that superluminal effects in amplifying media will be observed over the longest distances when the pulse’s spectrum has

little spectral content near the resonance. In absorbing media, as mentioned above, superluminal effects will persist longest for pulses with the least spectral content away from resonance. This is why narrowband pulses are generally used in both amplifying and absorbing experiments designed to observe these effects. Another technique was proposed by Bolda et. al. [9] which allows for longer superluminal propagation distances in amplifying media. They proposed to initially send the pulse through an absorbing medium to remove the near-resonance components from the pulse spectrum. This modified pulse is then sent through an amplifier with the same resonance frequency as the absorber. Since the slow near-resonance spectral components were attenuated in the absorber, a relatively large propagation distance is required before they enter into the expectation (28). (Of course there is no free lunch here: the extra long delay time in the absorber counterbalances the short delay time in the amplifier.)

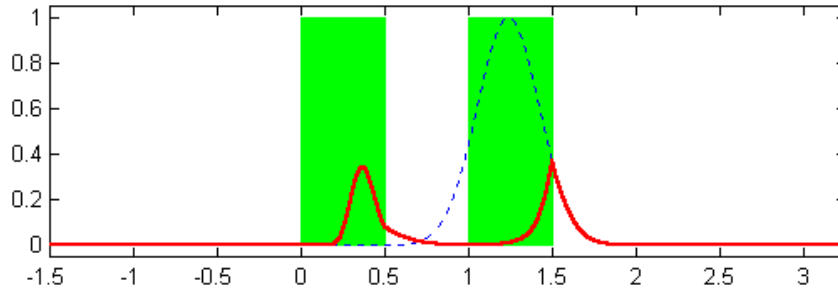


Fig. 8. Animation of a gaussian pulse traversing an absorbing medium followed by an amplifying medium as proposed by Bolda [9] (1.7 MB)

Figure 8 reproduces a time sequence of the spatial distribution of field energy which appeared in the article describing the experiment proposed by Bolda. Again, a dashed pulse is shown which propagates at exactly  $c$  (i.e. as if the absorber and amplifier were not there). The Lorentz model is used for the two media with  $\omega_0 = 2 \times 10^7 \gamma$ ,  $\omega_p = 100\gamma$ , and  $\Delta r = 0.5c/\gamma$ . The oscillator strength is  $f = 1$  for the absorbing medium and  $f = -1$  for the amplifier. The pulse is chosen to be gaussian as above with  $\tau = 0.264/\sqrt{2}\gamma$  and  $\bar{\omega} - \omega_0 = \omega_p/3$ .

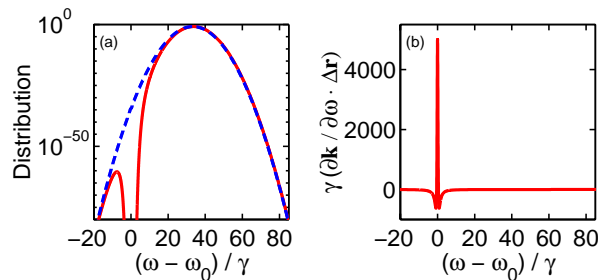


Fig. 9. (a) Spectral distribution before (dashed) and after (solid) traversing the absorber. The distribution after the amplifier is the same as the initial distribution. (b) Group delay function for the amplifying medium.

Figure 9(a) plots the spectral distribution of the pulse at different points in the medium. Figure 9(b) shows the group delay function for the amplifying medium. As usual, the delay time is predicted by the expectation of the group delay function weighted by the spectral distribution. (In the amplifying medium the reshaping delay  $\Delta t_R$  also plays a role since the pulse was chirped in the absorber. The reshaping delay is still small, however, amounting to about a 5% correction to  $\Delta t_G$ .) Because the near-resonance spectral components were removed, the large values of the group delay function near

resonance do not play a role in the expectation. Thus, the pulse passing through the amplifier can exhibit superluminal behavior over a relatively long distance. If the full gaussian is sent through the amplifier without this preparation, superluminal behavior persists over a displacement of only  $\Delta r = 7 \times 10^{-3}c/\gamma$  before becoming subluminal (and experiencing extreme amplification). This transition occurs when the amplitude of the on-resonance peak in  $\rho(\mathbf{r}, \omega)$  has roughly the same amplitude as the peak at the carrier frequency  $\bar{\omega}$ .

In addition to providing an example of how superluminal behavior can be extended over longer displacements, the Bolda example discussed above demonstrates the elegance and utility of the result (27). In Ref. [9] the prediction of a negative delay time is made using the traditional series expansion approach. The analytic motivation for introducing the absorber is simply that “frequencies very close to resonance are amplified by the gain medium to such an extent that the power-series expansion breaks down.” The new context gives clear insight into the physical reasons why the power series approach cannot be used to describe the pulse in the amplifier without first sending it through the absorber. If the unabsorbed pulse were sent into the amplifier, as the near-resonance frequency components were added to the pulse its velocity would change rapidly from superluminal to highly subluminal (as in fig. 7). Since the expansion terms evaluated at a single carrier frequency are useful to describe roughly constant velocity, they fail to describe the situation.

## 6 Conclusion

To summarize, we have found a context wherein the group delay function always retains meaning in a uniform linear medium. The results apply to pulses of arbitrary bandwidth and temporal complexity, even in the presence of anomalous dispersion where the pulse shape can evolve dramatically during propagation. The formalism distinguishes the roles of group velocity and spectral reshaping in determining total delay time. The net group delay is averaged over the final spectrum after the propagation takes place. The reshaping delay or displacement is the effect of eliminating from (or adding to) the original pulse the spectral amplitude that is lost (or gained) during propagation. This formalism does not attempt to identify a specific velocity as being representative of the overall pulse propagation as can be done for narrowband pulses. Rather it shows that a linear superposition of the group delays is necessary to determine total delay time.

We have illustrated the use of this formalism in situations where electromagnetic pulses propagate with superluminal delay times. We note that the formalism tracks the temporal ‘center of mass’ of the arrival of a pulse’s *electromagnetic field energy* only. It is important to realize that a superluminal delay time for the field energy center of mass does not require superluminal energy transport. For example, energy stored in the medium downstream from a pulse’s centroid may convert to field energy. The appearance of downstream field energy can make the pulse’s center of mass move superluminally while no actual energy transport occurs faster than  $c$ . In the absorbing case, the medium can preferentially absorb the trailing portion of a pulse, resulting in an advance of the pulse’s center of mass. In both of these cases the medium treats the leading and trailing portions of the pulse differently. In a companion article [17], we discuss why dielectric media behave in this manner as well as addressing the issue of energy transport velocity.